



10-4-14

## OBSERVATION AND NUMERICAL ANALYSES OF DYNAMIC EARTH-PRESSURE OF IN-GROUND LNG TANKS

Nobuhiro KAIZU, Tadashi SUGI, Hiroshi KUWAHARA and Hideyo SUZUKI

Engineering Research Center, The Tokyo Electric Power Co., Inc.,  
Chofu, Tokyo, Japan

### SUMMARY

This paper describes mainly the earth pressure during an earthquake acting to the in-ground LNG tank. Based on the observation, loading patterns of dynamic earth pressure around the tank are both "one side compression and opposite side depression" and "compression of both side and depression of both side" during the quake, and the dynamic earth pressure on the walls are considered to have correlation with the relative displacement between the tank and surrounding ground. According to numerical studies, the calculated dynamic earth pressures by means of aseismic design methods in Japan nowadays agree with observed ones.

### INTRODUCTION

In Japan, large number of cylindrical in-ground tanks with capacities of more than 60,000KL have been constructed in soft ground in order to store liquefied natural gas, in recent years. Construction of in-ground LNG tanks have been made possible by means of comprehensive studies such as numerical analyses, model experiments and earthquake observations (Refs. 1,2). However observation records of the earth pressure during earthquakes acting to those structures were limited in number (Ref. 3).

This paper describes the response behavior of dynamic earth pressure on the wall of in-ground LNG tank based on the observation data, together with numerical studies of dynamic behavior and some considerations of aseismic design methods, i.e. seismic coefficient method, seismic deformation method and axisymmetric dynamic finite element method, used in Japan nowadays.

### OBSERVATION SITE AND SYSTEM

The observation site is located in LNG Storing Station facing to Tokyo Bay about 40 km south part from Central Tokyo, as shown in Figure 1. There are six tanks in the Station. The in-ground LNG tank used for observation is cylindrical shaped reinforced concrete structure with diameter of 69.4 m, and the diaphragm wall 1.2 m in width holds a position at a distance of 3 m from the side wall, as shown in Figure 2. The upper part of the surrounding ground from AP +12.0 m to AP -4.0 m and the gap between the side wall and diaphragm wall is filled by sand.

Measuring instruments, i.e. earth pressure meter, acceleration meter and pore water pressure meter, are installed in/on the ground and on the wall of No.3 tank, as shown in Figure 2. The earth pressure meter is differential-transformer type, whose measuring capacity range is 50 or 100 tf/m<sup>2</sup>. All the acceleration

meters are magnetic force balance type, whose frequency range for sensitivity decrement within 5% are from 0.1 to 30.0 Hz. One of the acceleration meters at the point A3, in Figure 2, is installed in the same depth as the bottom of the tank. The acceleration meters of F point, in Figure 1, are installed in/on the free field ground at a distance of 100 m from No.1 in-ground tank.

#### OBSERVATION RESULTS AND CONSIDERATIONS

The earthquake concerned in this paper is Southern Ibaragi Prefecture Earthquake on October 4, 1985, JMA magnitude of 6.1, and epicentral distance is about 70 km, as shown in Figure 1.

The observed X component acceleration records and its fourier spectra are shown in Figure 3 and 4. There are the records in/on the free field ground, on the surrounding ground of No.3 tank and on the top of No.3 tank side wall. As in Figure 3, a maximum acceleration record on the free field ground was 45.4 gals. As in Figure 4, 2.8Hz is the predominant frequency of the acceleration wave on the side wall of No.3 tank, and its frequency agrees with the predominant frequency on the surrounding ground surface.

Figure 5 shows the observed dynamic earth pressure records at  $0^\circ$  direction of No.3 tank, pore water pressure record near the diaphragm wall at the  $0^\circ$  direction and relative displacement between the top of No.3 tank side wall and point A3 on the surrounding ground surface. A maximum dynamic earth pressure on the diaphragm wall was  $1.7\text{tf/m}^2$ . As in Figure 5, the frequency, phase and active direction of the dynamic earth pressure wave agree with those of relative displacement wave. These results of observation suggest an adequate correlation between the dynamic earth pressure on the wall and relative displacement. Similarly the frequency, phase and active direction of the dynamic earth pressure record on the diaphragm wall agree with those of the pore water pressure near the diaphragm wall. A maximum value of the difference between the dynamic earth pressure wave and pore water pressure wave is about  $1.2\text{tf/m}^2$ .

Figure 6 shows the vertical distribution of the dynamic earth pressure on the wall at  $0^\circ$  direction and relative displacement between No.3 tank and surrounding ground. It is considered that the dynamic earth pressures on the side wall, which are observed inside the diaphragm wall, are smaller than pressures on the upper part of the side wall, because of the presence of the diaphragm wall, and that the active direction of dynamic earth pressure agrees with the direction of relative displacement.

Figure 7 (a), (b) show the dynamic earth pressure records on the side wall at the  $90^\circ$  direction and at the  $270^\circ$  direction, time history of the product of these two waves and locus diagram between these two waves. As in these figure, it is noticed that there are two loading patterns during earthquake. A loading pattern of the dynamic earth pressure is "one side compression and opposite side depression" until about 18 second, but there appears "compression of both side and depression of both side" after 18 second.

#### NUMERICAL SIMULATION OF DYNAMIC EARTH PRESSURE

Some numerical studies of the dynamic earth pressure were performed by means of seismic coefficient method, seismic deformation method and axisymmetric dynamic finite element method currently, which are aseismic design methods used in Japan nowadays.

Seismic Coefficient Method The seismic coefficient method concerns the increment of earth pressure during earthquake determined by the seismic earth pressure formula of Dr. Okabe (Ref. 4).

In this case, the horizontal seismic coefficient is calculated based on the distribution of the acceleration records which are in/on the free field ground at point F in Figure 1.

The calculated dynamic earth pressures are shown in Figure 8. These agree approximately with the observed dynamic earth pressures except those on the upper part of the ground.

Seismic Deformation Method The seismic deformation method consists of calculating the seismic deformation of ground by means of the free field response analysis and applying the deformation to act on the tank through the medium of the spring of the ground (Ref. 2).

In this case, the tank and diaphragm wall were modeled by cylindrical shell model which attaches the springs of the ground. These springs are calculated by means of FEM. The seismic deformation is calculated by integration of the product of maximum ground strain and ground thickness for each stratum. Maximum ground strains are calculated by means of SHAKE using the observed acceleration wave at the seismic foundation.

The results of calculation are shown in Figure 8. The calculated dynamic earth pressures are well simulated the phenomenon as follows: the dynamic earth pressures at the upper part of the ground are larger than pressures of lower part of ground, and the calculated dynamic earth pressure distribution agrees with the observed records.

Axisymmetric Dynamic Finite Element Method A finite element method on an axisymmetric structure with antisymmetric dynamic loading is used to calculate the one- $\Theta$  response of the cylindrical wall (Ref. 1). The energy-transmitting boundary were assumed that the side of finite element model is the viscous boundary, and that the base boundary, i.e. seismic foundation, is rigid base. The observed acceleration wave was used for calculation as the input wave at the rigid base.

The results of calculation are shown in Figure 8. The calculated dynamic earth pressures agree well with the recorded pressures, if compared with other calculating methods. It is noticed that the dynamic earth pressures on the side wall inside the diaphragm wall are smaller than pressures on the upper part of the side wall, which are considered to be simulated by axisymmetric dynamic finite element method.

## CONCLUSION

According to the earthquake observations and some numerical studies, the behavior of dynamic earth pressure on the LNG tank wall was discussed. Major results of this studies are as follows.

- 1) Loading patterns of the dynamic earth pressure around the tank are both "one side compression and opposite side depression" and "compression of both side and depression of both side" during the quake.
- 2) The dynamic earth pressure on the wall during the quake are considered to have correlation with the relative displacement between the tank and surrounding ground.
- 3) The calculated dynamic earth pressures based on the ground deformation by means of SHAKE using the observed acceleration wave at the seismic foundation, are similar to the observed values.
- 4) The calculated dynamic earth pressures based on an axisymmetric model of FEM have sufficient accuracy, if compared with other calculating methods.

These results are obtained by means of the studies based on only one earthquake record such as maximum acceleration of 45.4 gals on the surface of free field ground. Further, it is necessary to accumulate the earthquake records and to study the dynamic earth pressure behavior during more large-scale earthquake that the ground behaves in non-linear region of materials.

## REFERENCES

1. Shirasuna, T., Goto, Y., "Response Behavior of Large-Scale Underground Tank During Earthquake," Proc. of 8WCEE, (1984).
2. Hamada, M., "Earthquake Observation and Numerical Analysis of a Large Underground Tank," Proc. of JSCE, No. 273, (1978).
3. Koyama, K., Watanabe, O., Kubota, T., Kusano, N., "Dynamic Behavior of LNG Inground Tank During Long-Period Earthquake," Proc. of 20th Annual Meeting of JSSMFE, E-8, (1985).
4. Committee on LNG Inground Storage, "Recommended Practice for LNG Inground Storage," Japan Gas Association, (1979).
5. Kuwahara, H., Kaizu, N., "Observations and Analyses of Seismic Responses of In-Ground LNG Tanks," Proc. of 7th JEES, (1986).

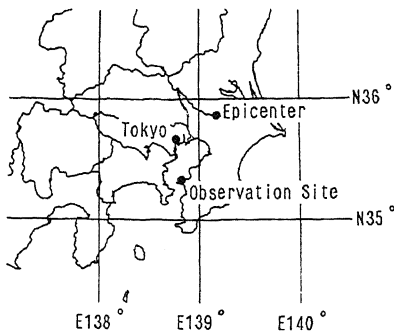


Fig.1 Location of Epicenter and Observation Site

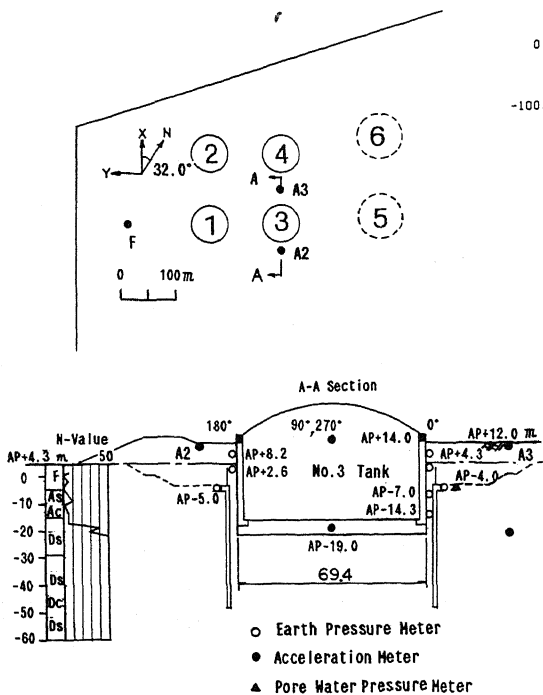


Fig.2 Location of Measuring Meters

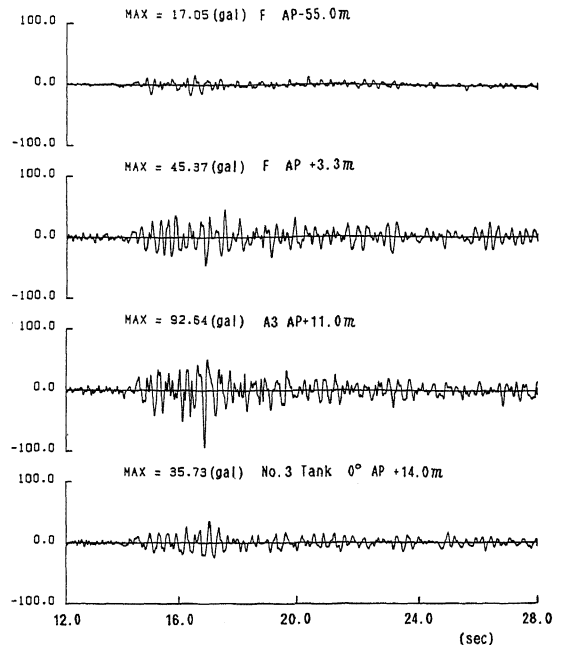


Fig.3 Acceleration Records (X-Direction)

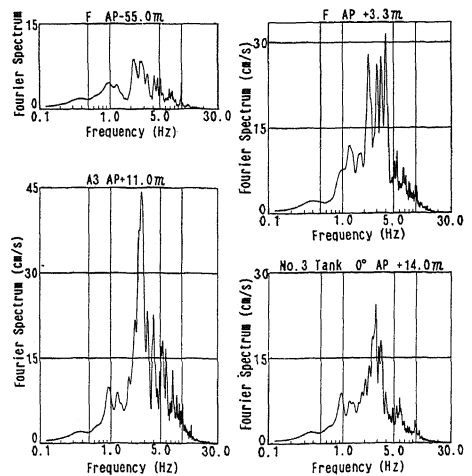


Fig.4 Fourier Spectra of Acceleration (X-Direction)

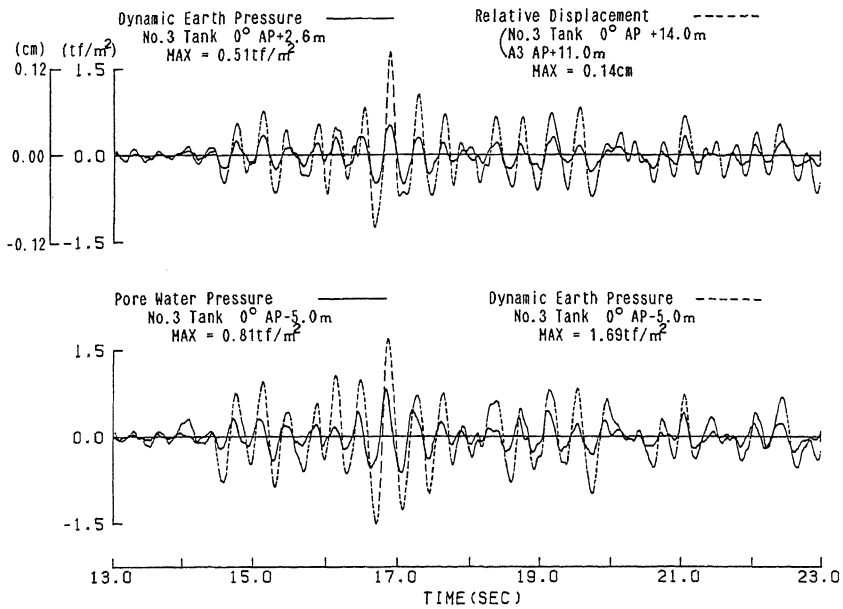


Fig.5 Dynamic Earth Pressure ,Pore Water Pressure and Relative Displacement Records (X-Direction)

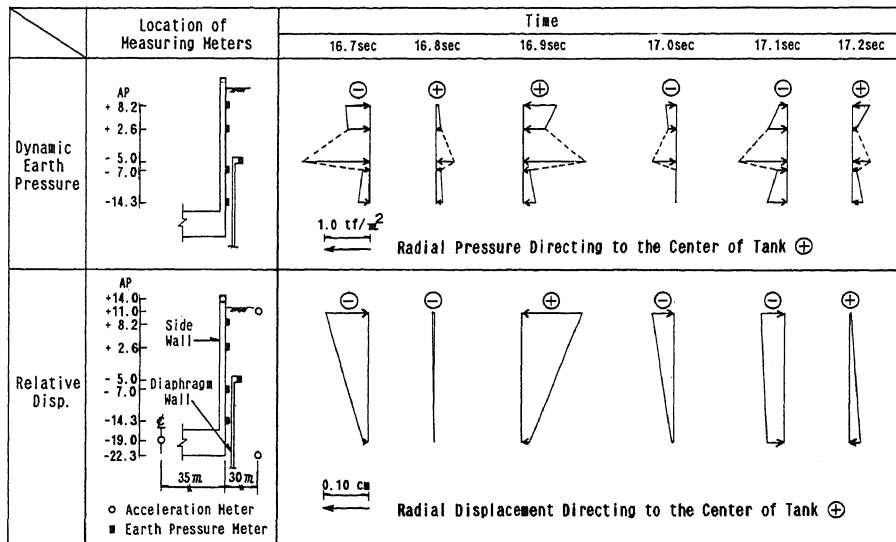


Fig.6 Relations between Dynamic Earth Pressure and Relative Displacement (X-Direction)

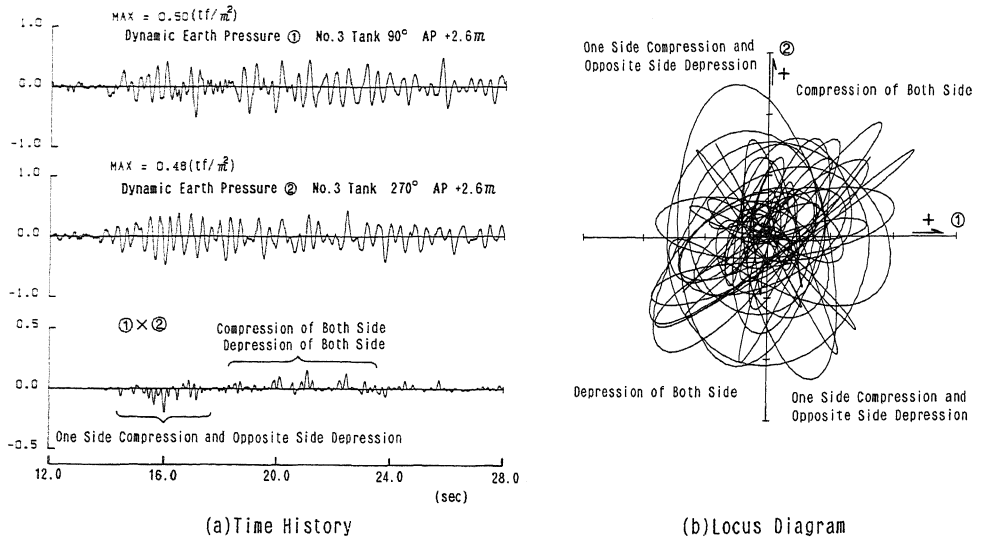


Fig. 7 Dynamic Earth Pressure Records (Y-Direction)

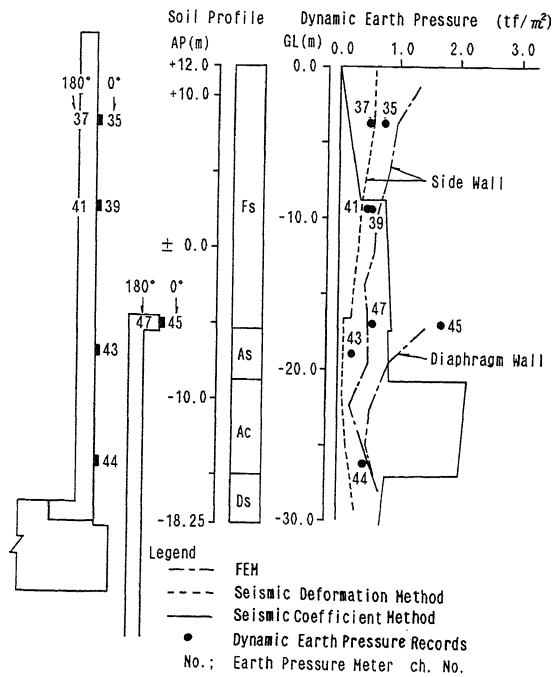


Fig. 8 Comparison between Recorded and Calculated Dynamic Earth Pressure (X-Direction)